

Open access • Journal Article • DOI:10.1038/380051A0

Rapid climate changes in the tropical Atlantic region during the last deglaciation

— Source link 

Konrad A Hughen, Jonathan T. Overpeck, Jonathan T. Overpeck, Larry C. Peterson ...+1 more authors

Institutions: University of Colorado Boulder, National Oceanic and Atmospheric Administration, University of Miami, University of California, Irvine

Published on: 07 Mar 1996 - Nature (Nature Publishing Group)

Topics: Thermohaline circulation, Younger Dryas, Deglaciation, Tropical Atlantic and Climate change

Related papers:

- Evidence for general instability of past climate from a 250-kyr ice-core record
- Holocene climatic instability: A prominent, widespread event 8200 yr ago
- Southward Migration of the Intertropical Convergence Zone Through the Holocene
- Deglacial changes in ocean circulation from an extended radiocarbon calibration
- Abrupt increase in Greenland snow accumulation at the end of the Younger Dryas event

Share this paper:    

View more about this paper here: <https://typeset.io/papers/rapid-climate-changes-in-the-tropical-atlantic-region-during-7d98depI33>

UC Irvine

UC Irvine Previously Published Works

Title

Rapid climate changes in the tropical Atlantic region during the last deglaciation

Permalink

<https://escholarship.org/uc/item/2d5484b0>

Journal

Nature, 380(6569)

ISSN

0028-0836

Authors

Hughen, KA
Overpeck, JT
Peterson, LC
et al.

Publication Date

1996-03-07

DOI

10.1038/380051a0

Copyright Information

This work is made available under the terms of a Creative Commons Attribution License, availalbe at <https://creativecommons.org/licenses/by/4.0/>

Peer reviewed

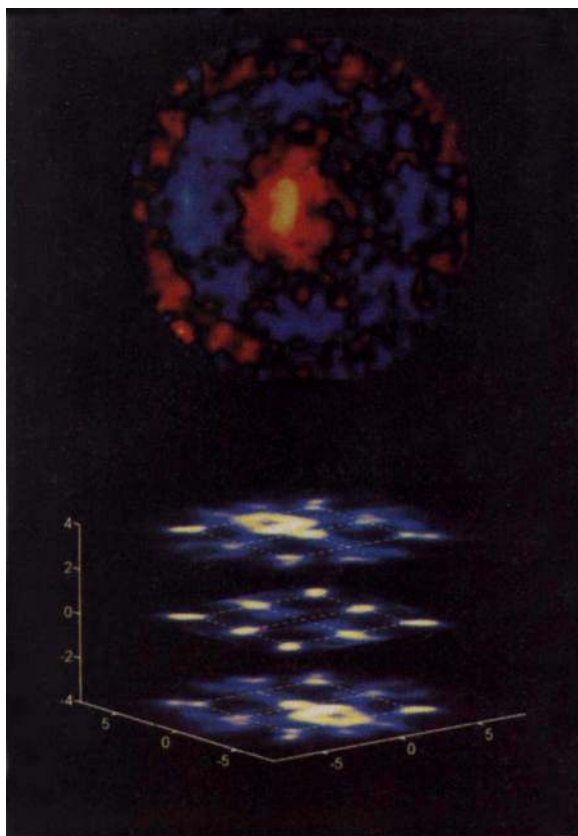


FIG. 2 Top panel, the hologram of SrTiO_3 after absorption correction and subtracting the contribution of the direct beam. This image is a projection of the spherical coordinates on the k_x - k_y (horizontal, vertical) plane ($k_x = \sin \theta \sin \phi$, $k_y = \sin \theta \cos \phi$; the definitions of θ and ϕ are given in Fig. 1). The radius of the hologram is 0.92. Bottom panel, three-dimensional holographic image of SrTiO_3 , showing only the Sr atoms (see text for details). The outline of eight elementary cells are shown by solid lines. The scale is given in Ångströms.

problem, and very promising methods have been developed^{12,17-19}. Here we do not use them as we intend to demonstrate that, without any *a priori* knowledge and a complicated evaluation procedure, the three-dimensional atomic order can be deduced. The different size of the atoms may be explained by the flat plate geometry. This geometry leads to different resolution in the plane which contains the source atom and is parallel with the crystal physical surface (in-plane), and in planes perpendicular to the crystal surface (out-of-plane). Because the diameter of the in-plane projection of the hologram is close to the maximum value of $2\pi/\lambda$, the in-plane resolution is $\sim 0.7 \text{ \AA}$ as expected from the wavelength of the fluorescent radiation. The out-of-plane resolution (almost 2 \AA) is determined by the size of the projection of the hologram to the direction perpendicular to the crystal surface, which is only about $(1/3)(2\pi/\lambda)$. Besides degrading the resolution, this also produces spurious oscillations in the reconstructed image. This problem could be overcome by using a small spherical sample instead of a flat one, and by recording the hologram on the full sphere. In this case the resolution would be the same in all directions. The effect of the above factors occur together and determine the final shape and size of the atoms in the reconstructed image.

We now consider future possibilities. Use of much brighter synchrotron sources for excitation, together with the development of fast one-dimensional high energy resolution detectors will allow the collection of much higher-quality data sets in a much shorter time. Therefore, in many cases our method might become a practical tool in solving the phase problem of single-crystal

diffractometry. A further step would be the development of advanced X-ray cameras with good energy resolution. Such cameras could follow, in real time, the dynamics of processes such as the change of atomic positions in a solid-solid phase transition. Our technique may also involve nuclear "inside" sources and scatterers. In a solid, excited nuclei can emit photons without recoil¹⁴ and with very well defined energy. These photons are elastically scattered not only by the electrons of the neighbouring atoms but also by the nuclei. The resonant nuclear scattering depends on the hyperfine fields in the sample. Therefore, one could obtain a three-dimensional picture of magnetic order or distinguish crystallographically equivalent atoms which sense non-equivalent electric field gradients or charge states. Further, the cross-section of nuclear scattering can be higher than that of the electronic charge scattering, resulting in an increased, isotope-selective sensitivity. □

Received 31 July 1995; accepted 24 January 1996.

1. Gabor, D. *Nature* **161**, 777–778 (1948).
2. Szöke, A. in *Short Wavelength Coherent Radiation: Generation and Applications* (eds Attwood, D. T. & Boker, J.) 361–467 (AIP Conf. Proc. No. 147, American Institute of Physics, New York, 1986).
3. Harp, G. R., Saldin, D. K. & Tonner, B. P. *Phys. Rev. Lett.* **65**, 1012–1015 (1990).
4. Thevuthasan, S. et al. *Phys. Rev. Lett.* **70**, 595–598 (1993).
5. Terminello, L. J., Barton, J. J. & Lapiano-Smith, D. A. *Phys. Rev. Lett.* **70**, 599–602 (1993).
6. Li, H., Tong, S. Y., Naumovic, D., Stuck, A. & Osterwalder, J. *Phys. Rev. B* **47**, 10036–10039 (1993).
7. Saldin, D. K., Harp, G. R. & Chen, X. *Phys. Rev. B* **48**, 8234–8244 (1993).
8. Han, Z. L. et al. *Surf. Sci.* **258**, 313–327 (1991).
9. Wei, C. M., Tong, S. Y., Wedler, H., Mendez, M. A. & Heinz, K. *Phys. Rev. Lett.* **72**, 2434–2437 (1994).
10. Tegez, M. & Faigel, G. *Europhys. Lett.* **16**, 41–46 (1991).
11. Maalouf, G. J., Hoch, J. C., Stern, A. S., Szöke, H. & Szöke, A. *Acta crystallogr. A* **49**, 866–871 (1993).
12. Len, P. M., Thevuthasan, S., Fadley, C. S., Kaduwela, A. P. & Van Hove, M. A. *Phys. Rev. B* **50**, 11275–11278 (1994).
13. Szöke, A. *Acta crystallogr. A* **49**, 853–866 (1993).
14. Mössbauer, R. L. Z. *Phys.* **151**, 124–143 (1958); *Naturwissenschaften* **45**, 538–539 (1958).
15. Barton, J. J. *Phys. Rev. Lett.* **61**, 1365–1359 (1988).
16. Saldin, D. K. & de Andrade, P. L. *Phys. Rev. Lett.* **64**, 1270–1273 (1990).
17. Chen, X. & Saldin, D. K. *Phys. Rev. B* **50**, 17463–17470 (1994).
18. Barton, J. J. *Phys. Rev. Lett.* **67**, 3106–3109 (1991).
19. Tong, S. Y. & Huang, H. & Wei, C. M. *Phys. Rev. B* **46**, 2452–2459 (1992).

ACKNOWLEDGEMENTS. This work was supported by OTKA and PHARE ACCORD.

Rapid climate changes in the tropical Atlantic region during the last deglaciation

Konrad A. Hughen*, Jonathan T. Overpeck*,†, Larry C. Peterson‡ & Susan Trumbore§

* INSTAAR and Department of Geological Sciences, University of Colorado, Boulder, Colorado 80309, USA

† NOAA Paleoclimatology Program, NGDC, Boulder, Colorado 80303, USA

‡ RSMAS, University of Miami, Miami, Florida 33149, USA

§ Department of Earth Systems Science, University of California, Irvine, California 92717, USA

THE climate system is capable of changing abruptly from one stable mode to another^{1–3}. Rapid climate oscillations—in particular the Younger Dryas cold period during the last deglaciation—have long been recognized from records throughout the North Atlantic region^{4–14}, and the distribution of these records at mostly high latitudes suggests that the changes were caused by rapid reorganizations of the North Atlantic thermohaline circulation^{6,8,10,15}. But events far from the North Atlantic region that are synchronous with the Younger Dryas^{16–19} raise the possibility that a more global forcing mechanism was responsible²⁰. Here we present high-resolution records of laminated sediments of the

last deglaciation from the Cariaco basin (tropical Atlantic Ocean) which show many abrupt sub-decade to century-scale oscillations in surface-ocean biological productivity that are synchronous with climate changes at high latitudes. We attribute these productivity variations to changes in or duration of upwelling rate (and hence nutrient supply) caused by changes in trade-wind strength, which is in turn influenced by the thermo-haline circulation through its effect on sea surface temperature^{6,21}. Abrupt climate changes in the tropical Atlantic during the last deglaciation are thus consistent with a North Atlantic circulation forcing mechanism.

The Cariaco basin (10° – 40° N, 65° W) is an anoxic marine basin located within the trade-wind belt off the northern coast of Venezuela (Fig. 1). The climate of the Cariaco basin region has a large seasonal signal, controlled by the annual north–south migration of the Intertropical Convergence Zone (ITCZ) in the Atlantic Ocean. When the ITCZ is farthest south (winter), rainfall in the Cariaco basin area is at a minimum and strong trade winds blow along the coast, inducing Ekman upwelling. When the ITCZ moves north (summer), the trade winds and upwelling diminish and the rainy season occurs. This results in a seasonal alternation of a dry, upwelling season and a rainy, non-upwelling season^{21–23}. Sedimentation patterns within the Cariaco basin accurately follow the climate, with annual deposition of a lighter-coloured, plankton-rich layer, followed by a darker-coloured, terrigenous grain-rich layer. Sediment cores recovered from the basin have continuously laminated sediments from the surface to a depth radiocarbon-dated at 12.6 kyr before present (bp). Previous work with ^{210}Pb and historical records has confirmed that the laminae couplets over the last century are annually deposited varves²³.

The construction of a multiple-core varve chronology and laminae thickness records is time-consuming, and is still in progress. In order to construct more rapidly a continuous record of Cariaco basin variability, we measured relative reflectivity (grey scale) on fresh surfaces of four cores from near the centre of the basin (Fig. 2). Radiocarbon age control through the laminated interval is provided by 20 accelerator mass spectrometry (AMS) ^{14}C dates on monospecific samples of the planktonic foraminifer *Globigerina bulloides* from one of the cores (Fig. 2). A reservoir correction age of 420 years was calculated for the Cariaco basin using two ^{14}C dates on near-surface sediments of precisely known age²³. This reservoir correction may have changed through time as a result of changes in upwelling and trade-wind strength. However, these two factors influence reservoir age in opposite directions, and the present value is close to that of the non-upwelling, open Atlantic (\sim 400 years), indicating the changes may have been small. Detailed correlations between the cores, independent of the grey-scale data, were made using individual ‘marker’ laminae observed in photographs, X-radiographs and petrographic thin sections. The cores display nearly identical grey-scale records, even in fine detail, indicating that the changes reflect variable surface conditions over the Cariaco basin in general, and are not limited to single locations. Comparing grey scale to a preliminary thickness record for the light-coloured, upwelling-season laminae from two of the cores shows that grey-scale values correlate well with average light-lamina thickness (Fig. 3). As light laminae increase in thickness, the sediments are more reflective and appear lighter, and vice versa. Slight disagreements in detail between the records may be due to the preliminary state of the lamina thickness record, which consists of 1-cm averages over much of its length. In general the agreement is good, suggesting that grey scale is controlled by the annual amount of biogenic productivity.

High-deposition-rate palaeoclimate records show that abrupt deglacial changes occurred across broad

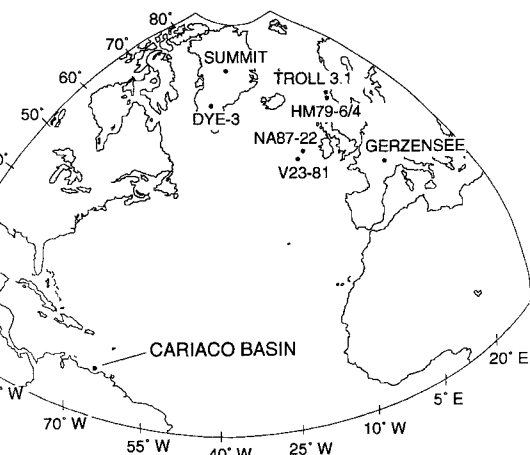


FIG. 1 Map of the North Atlantic region showing the location of the Cariaco basin in the western tropical Atlantic and the locations of high-latitude sites (referred to in the text) with records that correlate well with the productivity record of the Cariaco basin.

regions of the high-latitude North Atlantic. Dansgaard *et al.*⁹ showed synchronous changes of oxygen isotope ($\delta^{18}\text{O}$) records from the Dye-3 ice core in southern Greenland and calcite from Lake Gerzensee, Switzerland. Lehman and Keigwin¹⁰ correlated an abundance record of the polar foraminifer *Neogloboquadrina pachyderma* (sinistral) from marine core Troll 3.1 off the Norwegian coast to another *N. pachyderma* (s.) record from core V23-81 (Fig. 1), and correlated these with the Dye-3 and Gerzensee records. Koç-Karpuz and Jansen¹² showed similar deglacial changes in a spliced sea surface temperature (SST) record based on diatom assemblages from two marine cores, HM79-4 and -6, near core Troll 3.1 (Fig. 1). The same pattern of oscillations is repeated in $\delta^{18}\text{O}$ from ice cores at other Greenland sites, including Camp Century, Renland and Summit^{24–26}, as well as in snow accumulation, concentrations of several chemical species, and electrical conductivity from the GISP2 Greenland ice-core^{11,27,28}. Changes of the same character are also evident in $\delta^{18}\text{O}$ records

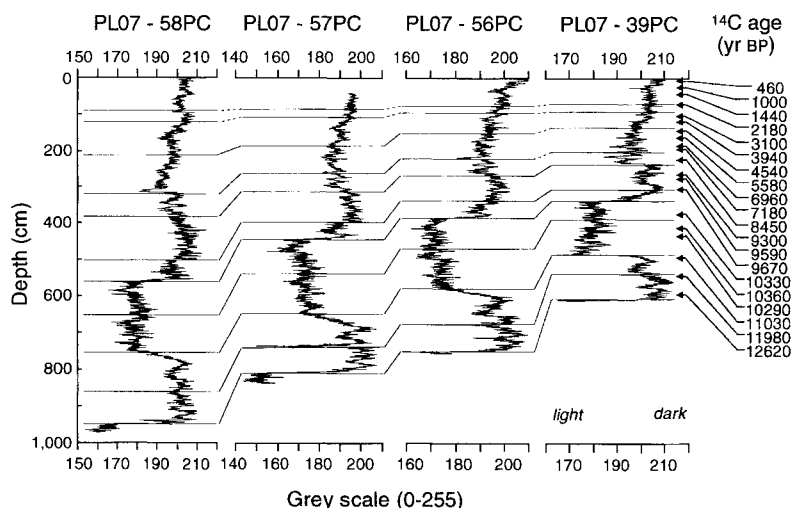


FIG. 2 Relative reflectivity (grey scale) from Cariaco basin cores PL07-58PC, -57PC, -56PC and -39PC. The correlation lines are based on individual laminae recognizable from photographs, X-radiographs and petrographic thin sections, and are intended as a check on grey-scale correlations. Age control is provided by 20 AMS ^{14}C dates on monospecific samples of the planktonic foraminifer *Globigerina bulloides* from core PL07-39PC, using a 420-year marine reservoir correction. The detailed pattern of grey-scale variability is clearly repeated in all cores. These data are archived at the World Data Center-A for Paleoclimatology (NOAA, Boulder, Colorado).

from the Faulensee (near Gerzensee) and Chirens bogs in the Swiss and French alps⁵, and in pollen curves from Lake Sandvikvatn, Norway⁷.

Together, these records clearly demonstrate that large areas of the high-latitude North Atlantic region experienced similar abrupt changes during the last deglaciation. The decade- to century-scale oscillations identified in these records correlate well with the grey-scale record of the tropical Cariaco basin (Fig. 4a). The Bølling/Allerød interval (14,500–12,500 calendar years BP, 14.5–12.5 cal. kyr BP)²⁹, for example, was interrupted by three decade- to century-scale events in each of these records. The events, from oldest to youngest, are named here the inter-Bølling cold period (IBCP), the Older Dryas (OD), and the inter-Allerød cold period (IACP), after refs 10 and 12. The Younger Dryas (12.5–11 cal. kyr BP) was an ~1,500-year-long interval of higher productivity in the Cariaco basin marked by abrupt transitions. Pollen records from the same latitude in Costa Rica indicate that temperature dropped by 2–3 °C at that time³⁰. The termination of the Younger Dryas in the Cariaco basin, estimated from thin sections of the varved sediments, occurred in less than a decade, in agreement with snow accumulation and other annual records from Greenland^{11,27,28}. Following the Younger Dryas termination was an oscillation during the Preboreal chron (PB) at 11 cal. kyr BP. After about 1,000 years, core PL07-56PC shows another series of oscillations, called early Holocene (EH), I, II and III, from 9 to 7.5 cal. kyr BP (Fig. 4a). EH III is clearly discernable in the Greenland record and changes at this time are seen in reconstructed sea surface conditions from foraminifera in North Atlantic core NA87-22 (ref. 14) and other records throughout the Atlantic basin^{21,31–34}. The Cariaco basin record shows continued variability throughout the rest of the Holocene, after 8 cal. kyr BP (Figs 2 and 4a).

The strong similarities between the Cariaco basin and GRIP records at the decade- to century-scale prompted us to compare

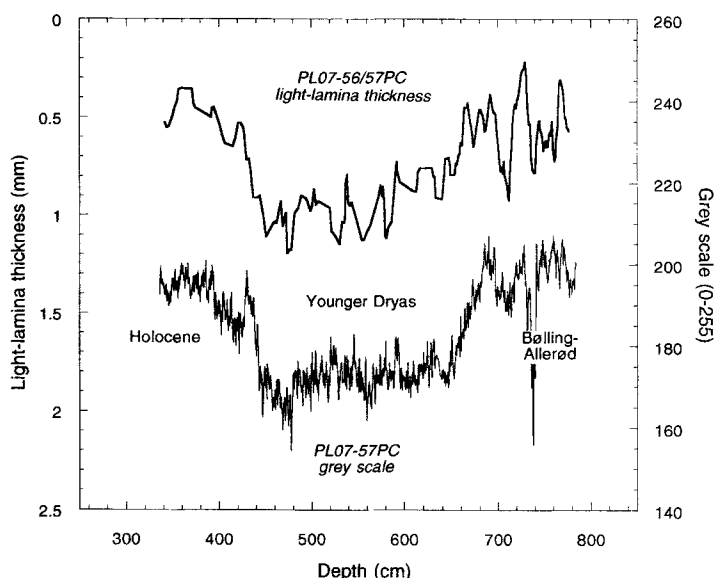
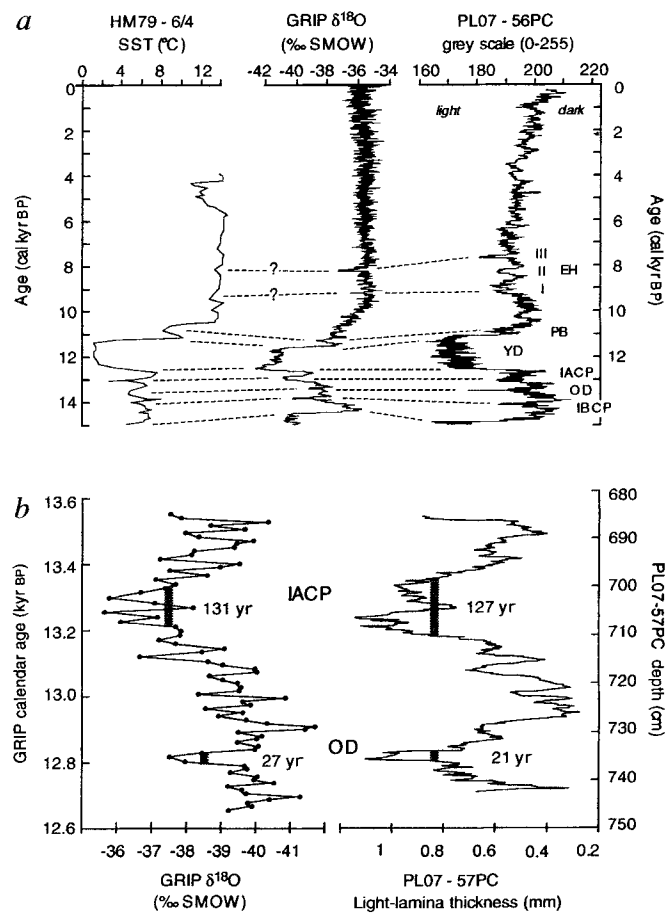


FIG. 3 Comparison of a preliminary spliced light-lamina-thickness record from cores PL07-56PC and -57PC to grey scale from core PL07-57PC. The thickness measurements, everywhere except during the Bølling/Allerød where they are annual (see Fig. 4b), are averages over 1-cm intervals and were made ~2–15 cm apart, depending on where thin sections were available for analysis. The large-scale excursions to brighter (low) values seen in the grey-scale record clearly coincide with increased average thickness of light laminae, and hence provide a proxy for changes in biogenic productivity.

these records at higher resolution. We compared a completed light-lamina thickness record from PL07-57PC to $\delta^{18}\text{O}$ data from GRIP over an interval including the inter-Allerød cold period and Older Dryas (Fig. 4b). Both records are constrained by annual chronologies, although the light-lamina record is smoothed with a 15-year running average and the GRIP core samples at this depth average 13–14 years together. The most negative $\delta^{18}\text{O}$ excursions seen in the GRIP record lasted approximately 131 and 27 years for the IACP and OD, respectively. The comparable events in the Cariaco basin were of similar duration, 127 and 21 years. In addition to the chronological agreement, there is also considerable similarity in the decade-scale patterns of variability in both records. Given the geographical distance separating central Greenland from the southern Caribbean Sea, the close match of the pattern and duration of decadal events between the two records is striking.

The similarity of detail between Cariaco basin and high-latitude North Atlantic records suggests a common forcing mechanism.

FIG. 4 a, Comparison of grey scale from Cariaco basin core PL07-56PC to $\delta^{18}\text{O}$ in the GRIP ice core²⁴ and August SST reconstructed from diatoms in lower-resolution marine cores HM79-6 and -4 (ref. 12). The Cariaco basin and HM79-6/4 records were converted to calendar ages for comparison to GRIP using the CALIB calibration program of Stuiver and Reimer²⁹. The comparison shows very similar patterns and timing of changes from 14–8 cal. kyr BP. Names of events are described in the text. b, Detailed comparison of $\delta^{18}\text{O}$ from the GRIP ice core²⁴ with changes in a continuous sequence of light-lamina thickness measurements from core PL07-57PC. Both records are constrained by annual chronologies, although neither record is sampled at annual resolution. The interval of comparison includes the inter-Allerød cold period (12.9–13 cal. kyr BP) and Older Dryas (13.4 cal. kyr BP) events (IACP and OD from a). The durations of the two events, measured independently in both records, are very similar, as is the detailed pattern of variability at the decadal timescale.

The brevity of the Older Dryas and other short events in Fig. 4b implies that the events occurred at nearly the same time. If there were a significant time lag (more than one wavelength of the briefest event) and signals would probably have been attenuated. The atmosphere has the geographic range and rapid response to link sub-decade changes in widely separated regions. Cariaco basin grey scale and light-lamina thickness record increases in primary productivity at times of cold in the North Atlantic. The most likely way to have increased productivity is to have increased intensity or duration of upwelling, in this case through strengthening of the trade winds. General circulation model results suggest that a reduction in North Atlantic SST would result in increased annually averaged trade winds over the tropical North Atlantic^{6,21}. This would cause an increase in Cariaco basin upwelling and productivity whenever North Atlantic SST was lowered. Thus it appears that shifts in North Atlantic thermohaline circulation, in addition to causing observed changes in high-latitude records, could have influenced trade-wind strength in the tropical Atlantic and caused the productivity record in the Cariaco basin.

The North Atlantic may have played a prominent role in controlling climate over most of the tropical Atlantic during the last deglaciation. Lake level records from northwestern Africa show periods of drought at about 11–10 and 8 ^{14}C kyr BP (refs 31–33), corresponding to the YD and EH intervals in the North Atlantic and Cariaco basin. These periods in the African records have been attributed partly to the influence of a cold North Atlantic on North African summer temperatures and monsoon precipitation^{31–33}. The similar timing of large changes in high- and low-latitude records may indicate a coupled tropical/high-latitude North Atlantic climate system operating during the last deglaciation until about 8 ^{14}C kyr BP. The mechanism for this coupling would be changes in North Atlantic SST influencing tropical Atlantic trade wind and summer monsoon strength. □

Received 24 July 1995; accepted 12 January 1996.

1. Manabe, S. & Stouffer, R. J. *J. Clim.* **1**, 841–866 (1988).
2. Broecker, W. S. & Denton, G. H. *Geochim. cosmochim. Acta* **53**, 2465–2501 (1989).
3. Stocker, T. F. & Wright, D. G. *Nature* **351**, 729–732 (1991).
4. Ruddiman, W. F. & McIntyre, A. *Palaeogeogr. Palaeoclimatol. Palaeoecol.* **35**, 145–214 (1981).
5. Siegenthaler, U., Eicher, U., Oeschger, H. & Dansgaard, W. *Ann. Glaciol.* **5**, 149–152 (1984).
6. Rind, D., Peteet, D., Broecker, W. S., McIntyre, A. & Ruddiman, W. *Clim. Dyn.* **1**, 3–33 (1986).
7. Paus, A. *Boreas* **17**, 113–139 (1987).
8. Broecker, W. S. et al. *Paleoceanography* **3**, 1–19 (1988).
9. Dansgaard, W., White, J. W. C. & Johnsen, S. J. *Nature* **339**, 532–534 (1989).
10. Lehman, S. J. & Keigwin, L. D. *Nature* **356**, 757–762 (1992).
11. Alley, R. B. et al. *Nature* **362**, 527–529 (1993).
12. Koç-Karpuz, N. & Jansen, E. *Paleoceanography* **7**, 499–520 (1992).
13. Bond, G. et al. *Nature* **365**, 143–147 (1993).
14. Duplessy, J. C. et al. *Nature* **358**, 485–488 (1992).
15. Broecker, W. S. et al. *Paleoceanography* **5**, 469–477 (1990).
16. Linsley, B. K. & Thunell, R. C. *Paleoceanography* **5**, 1025–1039 (1990).
17. Peteet, D. et al. *Eos* **75**, 587–590 (1993).
18. Denton, G. H. & Hardy, C. H. *Science* **264**, 1434–1437 (1994).
19. Thompson, L. G. et al. *Science* **269**, 46–50 (1995).
20. Broecker, W. S. *Nature* **372**, 421–424 (1995).
21. Overpeck, J. T., Peterson, L. C., Kipp, N., Imbrie, J. & Rind, D. *Nature* **338**, 553–557 (1989).
22. Peterson, L. C., Overpeck, J. T., Kipp, N. G. & Imbrie, J. *Paleoceanography* **6**, 99–119 (1991).
23. Hughen, K. A., Overpeck, J. T., Peterson, L. C. & Anderson, R. F. In *Paleoclimatology and Paleoceanography from Laminated Sediments* (ed. Kemp, A. E. S.) (The Geological Society, London, in the press).
24. Dansgaard, W. et al. *Nature* **364**, 218–220 (1993).
25. Johnsen, S. J. et al. *Nature* **359**, 311–313 (1992).
26. Grootes, P. M., Stuiver, M., White, J. W. C., Johnsen, S. & Jouzel, J. *Nature* **366**, 552–554 (1993).
27. Mayewski, P. A. *Science* **263**, 1747–1751 (1993).
28. Taylor, K. C. et al. *Nature* **361**, 432–436 (1993).
29. Stuiver, M. & Reimer, P. J. *Radiocarbon* **35**, 215–230 (1993).
30. Islebe, G. A., Hooghiemstra, H. & van der Borg, K. *Palaeogeogr. Palaeoclimatol. Palaeoecol.* **117**, 73–80 (1995).
31. Street-Perrott, F. A. & Perrott, R. A. *Nature* **343**, 607–612 (1990).
32. Lamb, H. F. et al. *Nature* **373**, 134–137 (1995).
33. Gasse, F. & Van Campo, E. *Earth planet. Sci. Lett.* **126**, 435–456 (1994).
34. Blunier, T., Chappellaz, J., Schwander, J., Stauffer, B. & Raynaud, D. *Nature* **374**, 46–49 (1995).

ACKNOWLEDGEMENTS. We thank C. Rooth, D. Murray and M. Kashgarian for valuable discussions and comments on the manuscript. We also thank H.-L. Lin for preparation of AMS ^{14}C samples for dating, and R. Spackman and M. Duval for help in the task of making thin sections. This work was supported by the US NSF and NOAA, as well as by NSF funding to the Lamont-Doherty Earth Observatory Deep-Sea Sample Repository.

Intense mixing of Antarctic Bottom Water in the equatorial Atlantic Ocean

K. L. Polzin*, K. G. Speer†, J. M. Toole‡ & R. W. Schmitt‡

* University of Washington, School of Oceanography, Box 357940, Seattle, Washington 98195, USA

† Laboratoire de Physique des Océans, IFREMER/CNRS, 29280 Plouzané, France

‡ Department of Physical Oceanography, Woods Hole Oceanographic Institution, Woods Hole, Massachusetts 02543, USA

THE SPREADING OF ANTARCTIC BOTTOM WATER—the densest global-scale water mass—is highly constrained by ocean-floor topography. In the Atlantic Ocean, the Mid-Atlantic Ridge confines this water mass mainly to the western basins, the bottom waters in the eastern basins being renewed by flows through gaps in the ridge¹. One such gap is the Romanche fracture zone, a large offset of the ridge which straddles the Equator. It has been observed² that sills within this fracture zone block the passage of waters colder than $\sim 0.9^\circ\text{C}$; warmer, less dense waters passing over the sills appear to cascade downslope where they are modified by mixing. Here we present direct measurements which quantify these processes. The flow is vertically sheared and exhibits remarkably intense turbulence, comparable to that seen at the ocean surface in the presence of winds of $\sim 10 \text{ m s}^{-1}$. This turbulence mixes the densest waters passing through the fracture zone with the warmer, overlying waters, so that the coldest waters exiting this region have been warmed by $\sim 0.6^\circ\text{C}$ during transit. Topographic obstructions and turbulent mixing together thus determine the properties of the flows renewing the deepest waters of the Atlantic Ocean's eastern basins.

Antarctic Bottom Water (AABW) represents a primary branch of the thermohaline circulation, the name given to the buoyancy-driven flow in the ocean. Bottom waters, created at high latitude when surface waters are made dense by heat loss and evaporation to the atmosphere, spread along the sea floor from their formation areas. In thermodynamic steady state, closure of the thermohaline circulation is accomplished by vertical mixing and upwelling. Mixing with warm overlying waters heats and lowers the density of the fluid at depth so that newly formed bottom waters can intrude below, forcing upward motion. The intensity of the mixing and its geographical distribution, as well as the causal physical mechanisms, have been subjects of great speculation in oceanography. Two conceptual models have been suggested: (1) nearly uniform modest-intensity mixing supported by internal wave breaking^{3,4} and (2) vigorous mixing only in close proximity to the sea floor, with subsequent horizontal distribution of mixing products into the relatively quiescent interior^{5,6}. In the second case, bottom boundary layer formation⁶ and breaking of bottom-reflected⁷ or bottom-generated⁸ internal waves have been suggested as possible mixing mechanisms. Recent studies have indicated only low-intensity turbulent mixing in the deep-ocean interior^{9,10}, arguing against (1). Here we explore a third scenario: that significant mixing occurs at bathymetric constrictions for the abyssal circulation.

The data for this study were obtained in November and December 1994 from the French research vessel *Le Noroit*. Our principal instrumentation consisted of the High-Resolution Profiler (HRP), a free-falling, internally recording profiler¹¹, and a conventional wire-lowered Conductivity–Temperature–Depth (CTD) instrument. The CTD returns estimates of the ocean's temperature and salinity variations with depth. The HRP adds horizontal velocity estimates and turbulent temperature and velocity gradient information. HRP profiles (28) and multiple CTD lowerings were made to depths as great as 5,300 m in the Romanche fracture zone (RFZ), two HRP stations were occupied